

## Self-organized quantum wires formed by elongated dislocation-free islands in (In,Ga)As/GaAs(100)

Wenquan Ma,<sup>a)</sup> Richard Nötzel,<sup>b)</sup> Achim Trampert, Manfred Ramsteiner, Haijun Zhu, Hans-Peter Schönherr, and Klaus H. Ploog  
*Paul-Drude-Institut für Festkörperelektronik, Hausvogteiplatz 5-7, D-10117 Berlin, Germany*

(Received 27 June 2000; accepted for publication 3 January 2001)

Long and fairly uniform quantum wire arrays have been fabricated by the growth of (In,Ga)As/GaAs multilayer structures. The structural properties of the quantum wires are characterized by atomic force microscopy, x-ray diffractometry, and transmission electron microscopy. The lateral carrier confinement in the quantum wires is confirmed by linear polarization dependent photoluminescence (PL) and magneto-PL measurements. © 2001 American Institute of Physics. [DOI: 10.1063/1.1352047]

Quantum dot and wire structures exhibit fascinating optoelectronic properties due to their modified density of states. Their fabrication has always been a challenge for crystal growth technology. Dislocation-free island formation was observed for Ge on Si(100)<sup>1</sup> and highly strained (In,Ga)As on GaAs(100).<sup>2</sup> This coherent Stranski-Krastanov growth mode has been applied to fabricate quantum dots, which are currently studied intensively. Tersoff and Tromp<sup>3</sup> predicted that elongated island formation, as an approach to the fabrication of quantum wires, is a universal property in strained systems. Their prediction was confirmed in CoSi<sub>2</sub> on Si(100).<sup>4</sup> Elongated island formation has been reported in systems such as for InAs/InP(100)<sup>5</sup> and (In,Ga)As/GaAs(100) with high In mole fraction.<sup>6</sup> However, for applications in optoelectronic devices, it is crucial to fabricate uniform and long quantum wires.

We report the formation of elongated (In,Ga)As islands on GaAs(100). Growth of (In,Ga)As/GaAs superlattice (SL) structures makes the islands more ordered and elongated. The structural properties are characterized by atomic force microscopy (AFM), transmission electron microscopy (TEM), and double crystal x-ray diffractometry (XRD). The lateral carrier confinement in the quantum wires is confirmed by linear polarization dependent photoluminescence (PL) and magneto-PL measurements.

All samples are grown on semi-insulating GaAs(100) substrates with miscut smaller than 0.05° by conventional solid source molecular beam epitaxy. The samples comprise three 15-period (In,Ga)As/GaAs SL structures with In mole fractions of 0.25, 0.17, denoted as SL25, SL17, respectively. The thicknesses of the (In,Ga)As and GaAs layers in the SLs are 1.8 and 19 nm, respectively. The growth rate of GaAs is 0.2350 μm/h and the As to Ga flux ratio is about 5. The GaAs buffer layer with thickness of 110 nm is grown at 580 °C. After the growth of each (In,Ga)As layer at 540 °C, 3 ML of GaAs are deposited at 540 °C without growth interruption to suppress the In segregation, then the substrate is heated up to 580 °C for GaAs growth. Finally, a 1.8 nm

(In,Ga)As top layer is grown for the observation of the surface morphology by AFM. The growth rate and In mole fraction for the three samples are calibrated by x-ray scans around symmetric (400) and asymmetric (422) reflections, showing the growth is coherent.

Figures 1(a) and 1(b) depict the AFM images of samples SL25 and SL17, respectively, revealing arrays of laterally periodic wire-like islands oriented along the  $[0\bar{1}1]$  direction. Most islands of the two samples are longer than 3 μm. The islands in Fig. 1(a) are comprised of dots arranged very closely along the  $[0\bar{1}1]$  direction, while those in Fig. 1(b) show a more uniform contrast. For comparison, we have grown 1.8 nm thick (In,Ga)As single layers with the same In source temperatures as samples SL25 and SL17, respec-

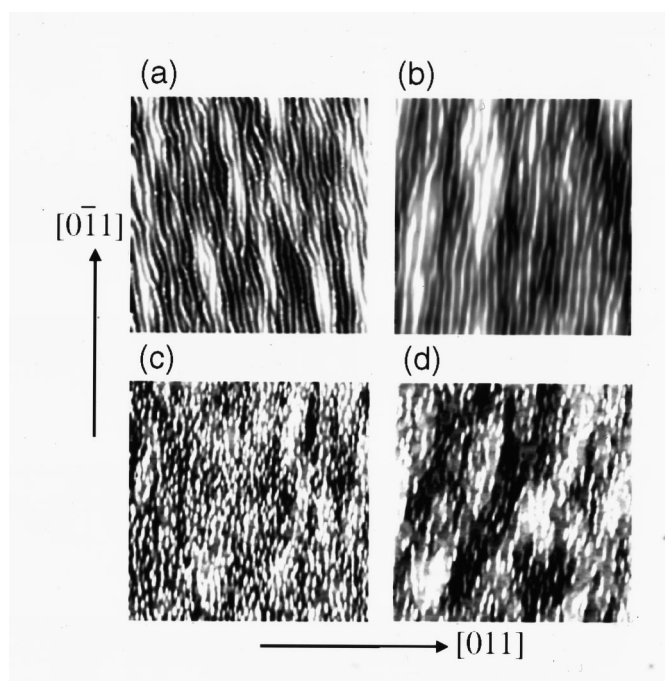


FIG. 1. (a) and (b) are AFM images of samples SL25 and SL17 (In mole fractions of 0.25 and 0.17), respectively; (c) and (d) are AFM images of the 1.8 nm thick (In,Ga)As single layer samples grown at 540 °C with the same In source temperatures as SL25 and SL17, respectively. The black-to-white height contrast of (a), (b), (c), and (d) is 15, 10, 3, and 3 nm, respectively. The scan range for all images is 5 μm × 5 μm.

<sup>a)</sup>Electronic mail: wqma@pdi-berlin.de

<sup>b)</sup>Present address: COBRA Interuniversity Research Institute, Eindhoven University of Technology, 5600 MB Eindhoven, The Netherlands.

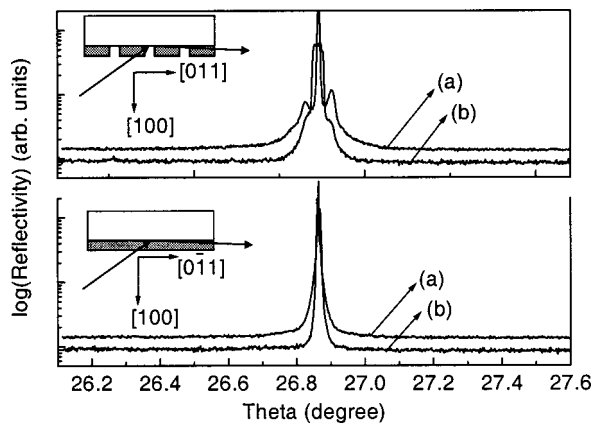


FIG. 2. Rocking curves of the (311) glancing exit reflection. The top (bottom) is measured for the x-ray beam perpendicular to (parallel to) the wire direction. (a) and (b) correspond to samples SL25 and SL17, respectively. The insets show the schematic diffraction geometry.

tively. AFM images [Figs. 1(c) and 1(d)] show slightly elongated islands distributed randomly, but the spacing between these cigar-like islands along the [011] direction is the same as the lateral period of the corresponding SL samples. To calibrate the In mole fraction of the single layer samples by XRD, we grew several SL samples at 540 °C continuously, showing that the In mole fractions corresponding to Figs. 1(c) and 1(d) are 0.35 and 0.28, respectively. This indicates that, during the growth of samples SL25, SL17, the heating of the substrate from 540 to 580 °C results in the desorption of In. Therefore, to get three dimensional islands with low In mole fraction, the heating of the substrate plays a role.

Because AFM images only show the topmost layer, we employ double crystal XRD and TEM measurements for samples SL25 and SL17 to get detailed information on the layered structure. XRD of a laterally periodic modulated structure can be regarded as multiple-slit Fraunhofer diffraction.<sup>7,8</sup> If an asymmetric diffraction is selected, XRD is very sensitive to the laterally periodic modulation due to the enhanced coherence. Figures 2(a) and 2(b) show x-ray rocking curves of the (311) glancing exit reflection for samples SL25 and SL17. When the x-ray beam is parallel to the  $[0\bar{1}1]$  direction, i.e., the wire direction, only the substrate peak appears. On the other hand, for the x-ray beam perpendicular to the wire, three satellite peaks are visible with one of them having the same position as the substrate. This confirms that the laterally periodic modulation exists in the whole epilayer stack. The satellite peaks are due to the interference induced by different slits (different gratings), therefore, the lateral period can be directly determined from the spacings between the satellites. The obtained values of 145 and 188 nm for samples SL25 and SL17, respectively, imply that the lateral periodicity is related to the In mole fraction. Considering that XRD averages over a relatively large volume, the appearance of the satellites indicates that the lateral periodicity of the two samples is fairly uniform.

Figures 3(a) and 3(b) [Figs. 3(c) and 3(d)] show the bright field cross-sectional TEM images taken in the  $[0\bar{1}1]$  and the  $[011]$  projections of sample SL17 (SL25), respectively. The images clearly reveal that the wires are vertically aligned. For sample SL17 [Fig. 3(a)], the lateral periodicity of the wires starting from the first layer is nearly as uniform

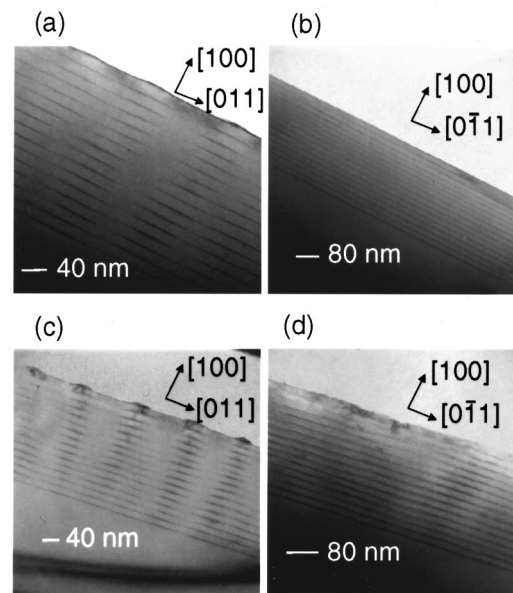


FIG. 3. (a) and (b) are the cross-sectional TEM images taken in the  $[0\bar{1}1]$  and  $[011]$  projections of SL17, respectively. (c) and (d) are those of SL25.

as that of the other stacked wires. The lateral periodicities of both samples determined by TEM are in agreement with those obtained by XRD and AFM measurements. The TEM image of SL17 taken in the  $[011]$  projection [Fig. 3(b)] shows a uniform SL structure. For sample SL25 [Fig. 3(d)], some nonuniformity occurs, which is probably due to the wiggle of the wire along the  $[0\bar{1}1]$  direction.<sup>9</sup> Further TEM investigations were carried out, where the samples were tilted against the  $\langle 011 \rangle$  zone axes, i.e., the (In,Ga)As/GaAs interface was inclined to the electron beam, demonstrating the absence of any dislocations from the first layer to the top layer in sample SL17. For sample SL25, no dislocations are detected in the 13 layers from the bottom, however, in some parts of the top three layers, stacking faults are found. These stacking faults may be due to the accumulation of strain in the top layers as compared to the bottom ones.

Island formation is favored at substrate locations where strain induces a local minimum of lattice mismatch. Therefore, the growth of a SL is a good scheme to generate a vertical correlation among islands if the thickness of the spacer layer is selected properly.<sup>10,11</sup> In Fig. 3(c), the islands in between the periodic wires in the initial layers are attributed to nucleation sites where the strain field is not at a distinct minimum.<sup>11</sup> Therefore, these intermediate islands disappear upon stacking more layers. The growth of a SL improves the uniformity of the wires and makes the wires much longer.

The question why the islands are elongated can be understood by Tersoff and Tromp's theoretical work.<sup>3</sup> In fact, we have already observed the existence of the shape transition, but a quantitative comparison with the theory is beyond the scope of this letter.

The crucial question whether or not carriers in the wire-like islands exhibit quantum confinement effects is investigated by PL spectroscopy. In Fig. 4, we show the linear polarization dependent PL spectra measured at 10 K. The polarization anisotropy, defined as  $(I_{\parallel} - I_{\perp}) / (I_{\parallel} + I_{\perp})$ , is 34%, where  $I_{\parallel}$  and  $I_{\perp}$  denote the PL intensities with the

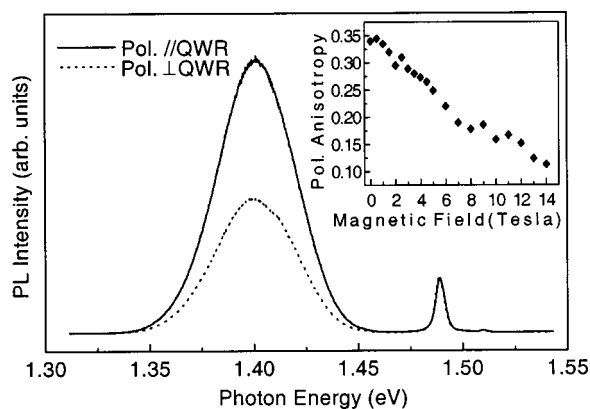


FIG. 4. Linear polarization dependent PL spectra of sample SL17. The inset displays the PL polarization anisotropy measured under magnetic field. The solid and dotted line are measured for detected polarization parallel and perpendicular to the wire direction, respectively. The peak at 1.490 eV is related to carbon acceptors in the substrate and the peak at 1.510 eV is related to bulk GaAs.

polarization parallel and perpendicular to the wire direction, respectively. However, the polarization anisotropy measurement itself is not a direct proof of lateral confinement in strained systems because the strain itself can cause a polarization anisotropy by modifying the valence band symmetry.<sup>12</sup> Magneto-PL measurement can distinguish between strain and lateral confinement induced polarization anisotropy. The polarization anisotropy induced by lateral confinement should decrease with decreasing the magnetic confinement length.<sup>13</sup> As shown in the inset in Fig. 4, with increasing the vertical magnetic field from 0 to 14 T (the maximum magnetic field available), the polarization anisotropy

decreases continuously from 34% to 11%, demonstrating that the polarization anisotropy is dominantly induced by the lateral confinement.

In summary, long and fairly uniform quantum wire arrays have been fabricated. The lateral carrier confinement in this wire structure has been confirmed by linear polarization dependent PL and magneto-PL measurements. Our work may experimentally pave a way to the fabrication of very long and uniform quantum wires.

The authors wish to thank O. Brandt and L. Däweritz for valuable discussions. Part of this work was supported by the Bundesministerium für Bildung und Forschung, and the NEDO NTDP-98 project.

- <sup>1</sup>D. J. Eaglesham and M. Cerullo, *Phys. Rev. Lett.* **64**, 1943 (1990).
- <sup>2</sup>S. Guha, A. Maduhkar, and K. C. Rajkumar, *Appl. Phys. Lett.* **57**, 2110 (1990).
- <sup>3</sup>J. Tersoff and R. M. Tromp, *Phys. Rev. Lett.* **70**, 2782 (1993).
- <sup>4</sup>S. H. Brongersma, M. R. Castell, D. D. Perovic, and M. Zinke-Allmann, *Phys. Rev. Lett.* **80**, 3795 (1998).
- <sup>5</sup>H. X. Li, T. Daniels-Race, and Z. G. Wang, *J. Cryst. Growth* **200**, 321 (1999).
- <sup>6</sup>K. Tillmann, D. Gerthsen, P. Pfundstein, A. Förster, and K. Urban, *J. Appl. Phys.* **78**, 3824 (1995).
- <sup>7</sup>L. Tapfer, G. C. La Rocca, H. Lage, O. Brandt, D. Heitmann, and K. Ploog, *Appl. Surf. Sci.* **267**, 227 (1992).
- <sup>8</sup>L. De Caro, P. Sciacovelli, and L. Tapfer, *Appl. Phys. Lett.* **64**, 34 (1994).
- <sup>9</sup>N. S. Chokshi and J. M. Millunchick, *Appl. Phys. Lett.* **76**, 2382 (2000).
- <sup>10</sup>Q. Xie, A. Madhukar, P. Chen, and N. P. Kobayashi, *Phys. Rev. Lett.* **75**, 2542 (1995).
- <sup>11</sup>J. Tersoff, C. Teichert, and M. G. Lagally, *Phys. Rev. Lett.* **76**, 1675 (1996).
- <sup>12</sup>I. Vurgaftman and J. Singh, *J. Appl. Phys.* **77**, 4931 (1995).
- <sup>13</sup>M. Notomi, J. Hammersberg, J. Zeman, H. Weman, M. Potemski, H. Sugiura, and T. Tamamura, *Phys. Rev. Lett.* **80**, 3125 (1998).